

A label-free lateral offset spliced coreless fiber MZI biosensor based on hydrophobin HGFI for TNF- α detection*

WANG Bo¹, DUAN Shaoxiang², ZHANG Hao², XU Haijin¹, LIU Bo^{2**}, and QIAO Mingqiang^{1,3**}

1. The Key Laboratory of Molecular Microbiology and Technology, Ministry of Education, Nankai University, Tianjin 300071, China

2. Institute of Modern Optics, Tianjin Key Laboratory of Optoelectronic Sensor and Sensing Network Technology, Nankai University, Tianjin 300350, China

3. School of Life Science, Shanxi University, Taiyuan 030006, China

(Received 13 April 2022; Revised 24 April 2022)

©Tianjin University of Technology 2022

A real-time label-free lateral offset spliced coreless fiber (CF) Mach-Zehnder interferometer (MZI) biosensor functionalized with hydrophobin *Grifola frondosa* I (HGFI) was proposed for the detection of cytokine tumour necrosis factor alpha (TNF- α). The nanolayer self-assembled on the optical fiber surfaces by HGFI rendered the immobilization of probe TNF- α antibody and recognition of antigen TNF- α . Trifluoroacetic acid was utilized to remove the HGFI layer from the glass surface, which was validated by field emission scanning electron microscopy (FESEM) and water contact angle (WCA). Results demonstrated that the processes of HGFI modification, antibody immobilization and specific antibody detection can be monitored in real time. The proposed biosensor exhibited good specificity, repeatability and low detection limit for TNF- α , extending its application in inflammation and disease monitoring.

Document code: A **Article ID:** 1673-1905(2022)05-0263-6

DOI <https://doi.org/10.1007/s11801-022-2061-2>

Tumour necrosis factor alpha (TNF- α) is a pro-inflammatory cytokine that plays a key role in a variety of pathological processes^[1]. It is a crucial biomarker whose level in serum elevated in numerous diseases, such as rheumatoid arthritis^[2], Alzheimer's disease^[3], diabetes^[4] and cancers^[5]. Recently, there has been increasing interest in TNF- α detection and approaches, such as enzyme-linked immunosorbent assays^[6], chemiluminescence immunoassay^[7], electrochemical immunosensors^[8], have been thoroughly investigated. In contrast, fiber-optic biosensors have advantages in easily fabrication, low cost and high resolution, and have been widely applied for biochemical processes detection^[9-11].

The bio-probe molecules immobilization is considered as one of the most important steps of sensors fabrication. Various methods, such as electrostatic adsorption through the positive charge of Poly-L-Lysine (PLL) layer^[12], specific recognition through biotin-avidin system^[13], and covalent coupling with the sulfhydryl group introduced by (3-aminopropyl) triethoxysilane (APTES) silanization^[14], were employed for surface functionalization.

However, the lack of adsorption stability and the complexity of the reaction procedures severely limit their applicability and commercialization.

Hydrophobins are a series of amphipathic proteins that typically produced by filamentous fungus and can be self-assembly into nanolayers on the interfaces, altering surface wettability^[15]. In terms of hydrophobic patterns and characteristics of the film formed, hydrophobins are divided into two subgroups^[16]. Class I hydrophobins^[17] can generate highly stable films with rodlets morphology and are only disaggregated by strong acids like trifluoroacetic acid (TFA) and formic acid. Class II hydrophobins^[18] cannot form rodlets and their films can be disaggregated by 2% sodium dodecyl sulfate (SDS) and 60% ethanol. Properties of hydrophobins including low toxicity and high biocompatibility have led to their widespread applications in surface functionalization^[19] and drug delivery^[20].

The hydrophobin layer has been shown to adsorb proteins using both hydrophobic and electrostatic forces^[21]. In our previous researches, the hydrophobin *Grifola*

* This work has been supported by the Sino-Swiss Scientific and Technological Cooperation Project supported by the Ministry of Science and Technology of China (No.2015DFG32140), the National Key Research and Development Program of China (Nos.2018YFA0900100 and 2018YFB1802302), the National Natural Science Foundation of China (Nos.11774181, 11804250, 11904180, 11904262, 61875091 and 62105164), the Natural Science Foundation of Tianjin City (Nos.19JCYBJC16700, 20JCQNJC01480, 21JCQNJC00210 and 21JCYBJC00080), and the Tianjin Education Commission Scientific Research Project (Nos.2018KJ146 and 2019KJ016).

** E-mails: liubo@nankai.edu.cn; qiaomq@nankai.edu.cn

frondosa I (HGFI) had been employed to modify antibody probe on the surface of optical fiber to detect antibody-antigen interaction^[22-24]. These investigations suggested that HGFI was a viable option for TNF- α detection by TNF- α antibody immobilization. In this study, a label-free lateral offset spliced coreless fiber (CF) Mach-Zehnder interferometer (MZI) biosensor based on HGFI was fabricated to detect TNF- α in vitro.

Biomaterials used in this study include TNF- α neutralizing antibody (10602-MM0N1, sino Biological) as the probe, recombinant human TNF- α (10602-HNAE, sino Biological) as the target antigen, 2019-nCoV nucleocapsid protein (N protein, P2328, Beyotime) as a mismatch antigen, phosphate buffer saline (PBS) (0.01 mmol Na₂HPO₄, 0.15 mol NaCl, pH=7.4) and TFA (T6508, 99%, Sigma-Aldrich, Fluka). Hydrophobin HGFI was prepared as described previously^[25]. A fed-batch fermentation was carried out to produce HGFI by *Pichia pastoris* GS115-pPIC9K-hgfi. The supernatant fluids were harvested by centrifugation (8 000 r/min). The crude materials were purified by ultrafiltration and high efficiency liquid chromatography. The purified HGFI was lyophilized and redissolved in deionized water in 300 μ g/mL. The antibody and antigens were diluted with PBS to 5 μ g/mL for antibody and 1 μ g/mL for antigens, respectively.

The proposed lateral offset fiber-optic MZI (LOFMZI) was made by fusing single mode fiber (SMF) and CF structures with a lateral offset CF in a fiber splicer (Furukawa S178A, in a manual operation mode). A section of CF1 with cladding diameter of 125 μ m was spliced with the lead-in SMF and another section of CF3 was spliced with the lead-out SMF. CF was cleaved with designed length with the assistance of translation stage. Lateral offset CF2 was spliced with CF1 and CF3 with predesigned offset along *X* direction but laterally aligned along *Y* direction. The splicing parameters are as follows. The discharge electric intensity was 70 bit and duration time was 325 ms. The microscope photograph of LOFMZI sensor is presented in Fig.1. The lengths of CF1, CF2 and CF3 are 106.04 μ m, 600.60 μ m and 107.80 μ m, respectively. The lateral offset distance is 61.60 μ m.

When the light was launched through CF1, the beam would separate into two portions, which propagated through the lateral offset CF2 (*I*₁) and the cavity (*I*₂), as shown in the blue arrows in Fig.1, and then interfered at CF3. To investigate light propagation of our proposed sensor in air and water condition, simulation was utilized to analyze power evolution process based on the beam propagation theory, as illustrated in Fig.2. Due to the optical path difference between these two portions of light, interference would occur at the lead-out SMF, which was sensitive to the refractive index change of the cavity medium. The interference light intensity could be expressed as follows^[26]

$$I = I_1 + I_2 + 2\sqrt{I_1 I_2} \cos\left(\frac{2\pi\Delta n_{\text{eff}} L}{\lambda}\right), \quad (1)$$

where λ is the optical wavelength, Δn_{eff} is effective refractive index difference of the interference modes, and L is interference length. Therefore, interference fringe pattern dip appears at wavelength of

$$\lambda_{\text{dip}} = \frac{2\Delta n_{\text{eff}} L}{2m+1}, \quad (2)$$

where m is an integer. Local enrichment of protein on the fiber surface results in refractive index change. The dip wavelength changes with the refractive index variation of medium accordingly.

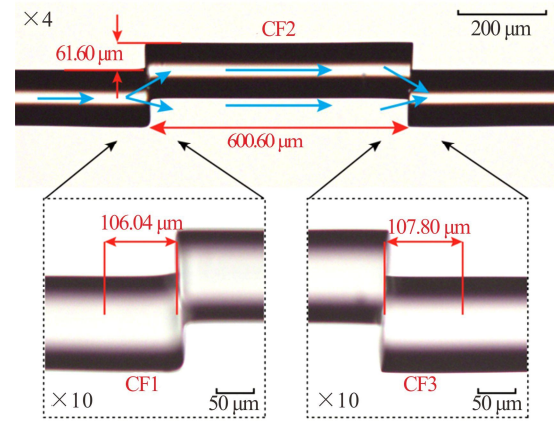


Fig.1 Micrographs of LOFMZI sensor (The magnified images (inset) of CF1 and CF3 regions are shown below)

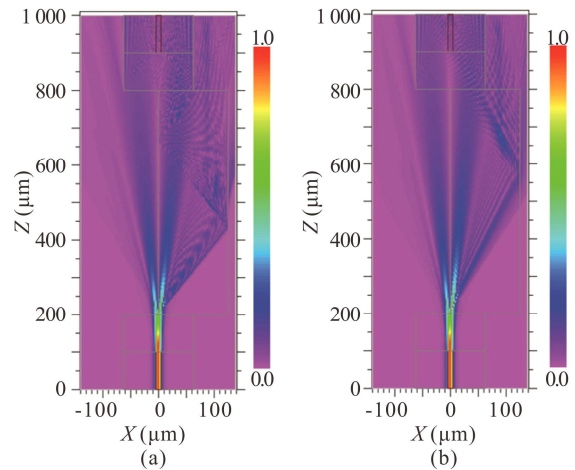


Fig.2 Simulation results of beam propagation process for the LOFMZI with different conditions of (a) air and (b) water

The experimental setup of HGFI functionalized MZI biosensor for TNF- α detection was schematically illustrated in Fig.3, which consisted of a supercontinuum broadband source (SBS) ranging from 1 250 nm to 1 640 nm, an optical spectrum analyzer (OSA, Yokogawa AQ6370D, operation wavelength ranges from 600 nm to 1 700 nm) with a wavelength resolution of 0.2 nm, an integrated microfluidic channel with inserted fabricated

LOFMZI sensor inside, poly tetra fluoroethylene (PTFE) tubes connected with a pressure syringe for samples pumping in, and a beaker for waste collection.

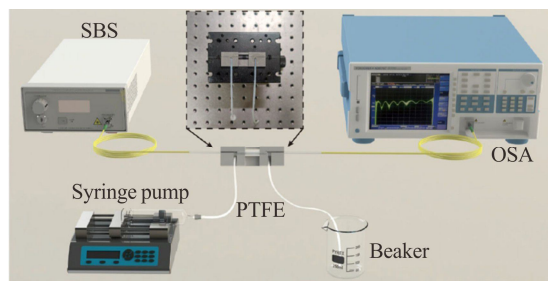


Fig.3 Schematic diagram of experimental setup for the TNF- α detection system

The processes of optical fiber modification and antigen detection were depicted schematically in Fig.4 and conducted as follows. HGFI solution was firstly pumped into the microfluidic channel and incubated for 15 min. TNF- α solution was then pumped into the microfluidic channel and incubated for 40 min, and antigen solution was finally pumped into the microfluidic channel and incubated for 40 min. All the dynamically incubation phases were carried out at room temperature (25 °C) with a flow rate of 0.1 μ L/min, and the microfluidic channel was washed repeatedly with deionized water to eliminate dissociative proteins between each step. The relative wavelength shifts in response to each process were recorded in real time.

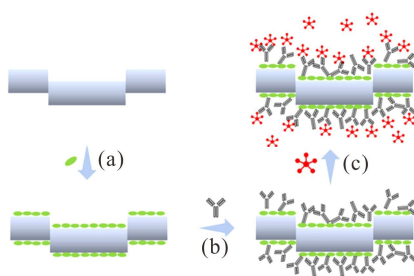
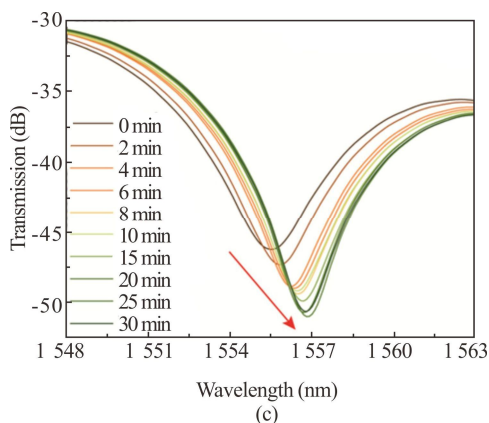
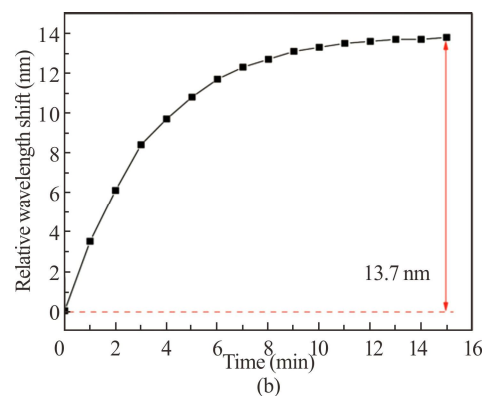
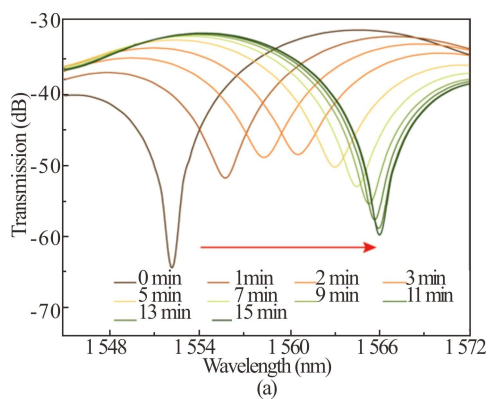


Fig.4 Schematic diagrams of the DNA hybridization procedure: (a) Surface functionalization of the LOFMZI by HGFI; (b) Immobilization of probe antibody; (c) Detection of target antigen with immobilized probe antibody

Fig.5 shows the corresponding transmission spectra and relative wavelength shifts for all processes. The resonant dip near 1 550 nm is selected to analyze processes of HGFI modification, TNF- α antibody immobilization and TNF- α detection. With the increase of time, the wavelengths were gradually stabilized, indicating reactions of HGFI self-assembly, antibody binding to HGFI and antigen recognition by antibody have reached saturation point. The wavelengths were red-shifted by 13.7 nm, 1.3 nm and 2.3 nm, respectively, indicating that this

LOFMZI sensor showed a detection limit less than 1 μ g/mL for TNF- α in PBS.

In order to analyze the specificity and repeatability of a single optical fiber in our system, all the biomaterials on the surface must be removed entirely. Herein, TFA was employed to remove the HGFI layer on the surfaces of original glass pieces. A 100 μ L drop of HGFI solution (300 μ g/mL) was added on the surface of a clean glass piece and evaporated at 60 °C. The HGFI-coated surface was then washed with 5 mL pure TFA and sufficient de-ionized water, successively. Field emission scanning electron microscopy (FESEM, SIGMA 500, ZEISS) images in Fig.6(a) and (b) suggested that a layer with rodlets morphology was observed on the surface of HGFI-coated glass, whereas no layer remained following TFA treatment, indicating that the HGFI layers were efficiently removed.



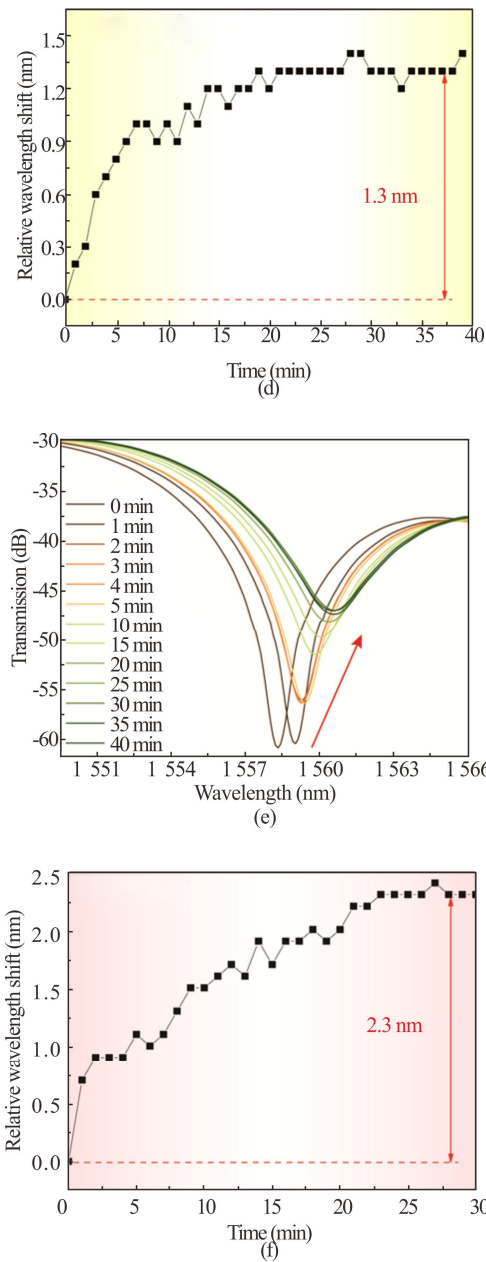


Fig.5 Corresponding transmission spectra and relative wavelength shifts for different steps: (a) and (b) HGFI modification; (c) and (d) TNF- α antibody immobilization; (e) and (f) TNF- α detection

A 100 μL drop of HGFI solution (300 $\mu\text{g}/\text{mL}$) was added on the surface of a clean glass piece and incubated in room temperature overnight. The modified surface was then rinsed with deionized water to remove any uncovered HGFI. 50 μL TFA was added and covered the modified region for 10 s, then removed by filter paper. Three times of TFA treatment were repeated and the surface was finally washed with deionized water. Water contact angle (WCA) was determined using CAM 200 compact contact angle meter system (KSV Instruments Ltd., Helsinki, Finland) and images in Fig.6(c) to (e) showed that the WCA of glass surface decreased from $37.4^\circ \pm 1.5^\circ$ to $9.2^\circ \pm 1.2^\circ$ after HGFI coating, indicating

that the surface became more hydrophilic as a result of HGFI modification. After TFA treatment, the WCA of HGFI modified glass surface increased back to $36.3^\circ \pm 1.7^\circ$, suggesting that the HGFI layer was successfully removed.

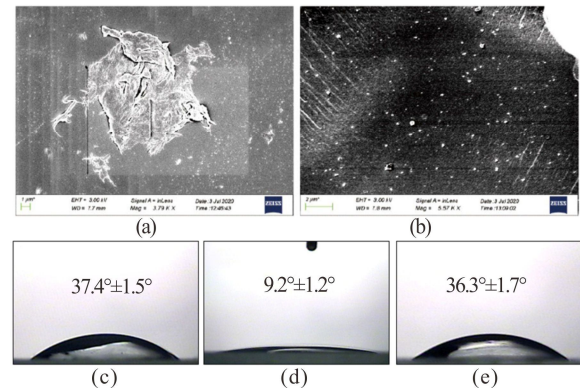


Fig.6 FESEM images of (a) HGFI modified glass surface and (b) HGFI modified glass surface followed by TFA treatment; WCA results on different glass surfaces: (c) Bare surface; (d) HGFI modified surface; (e) HGFI modified surface followed by TFA treatment

PTFE tubes were used in the setup and 1 mL pure TFA was pumped into the microfluidic channel with a flow rate of 200 $\mu\text{L}/\text{min}$ followed by washing with 5 mL ethanol (500 $\mu\text{L}/\text{min}$), 5 mL 0.2 mol/L NaOH solution (500 $\mu\text{L}/\text{min}$), and 5 mL deionized water (500 $\mu\text{L}/\text{min}$) to remove the residual TFA. Another two HGFI modification processes were repeated, and no significant difference was observed in relative wavelength shifts, as shown in Fig.7, indicating that the optical fiber can be repeatedly utilized to be modified with HGFI.

The HGFI remodified LOFMZI sensor was subsequently immobilized with TNF- α antibody probe as previously described. A mismatched antigen N protein of 2019-nCoV was utilized to test the specificity of our system. As shown in Fig.8, the transmission spectra only exhibit fluctuations of wavelength shift at a range of 0.3 nm when the sensor was exposed in N protein solution. Following TFA treatment and washing, an additional TNF- α detection procedure was carried out. As expect, a similar transmission dip response behavior was observed, indicating that the LOFMZI sensor fabricated in this study was reproducible for specific antigen detection with good repeatability. More broadly, the microstructure parameters of the sensor^[27] and probe immobilization conditions^[28] are needed to be optimized to elevate the detection sensitivity for biomarkers detection in serum or other biological samples, as well as shorten the time of surface modification.

In conclusion, a hydrophobin HGFI modified LOFMZI biosensor was developed and applied to detect the pro-inflammatory cytokine TNF- α in vitro. Results demonstrated that the probe TNF- α antibody was simply immobilized by HGFI layer, facilitating the repeatable

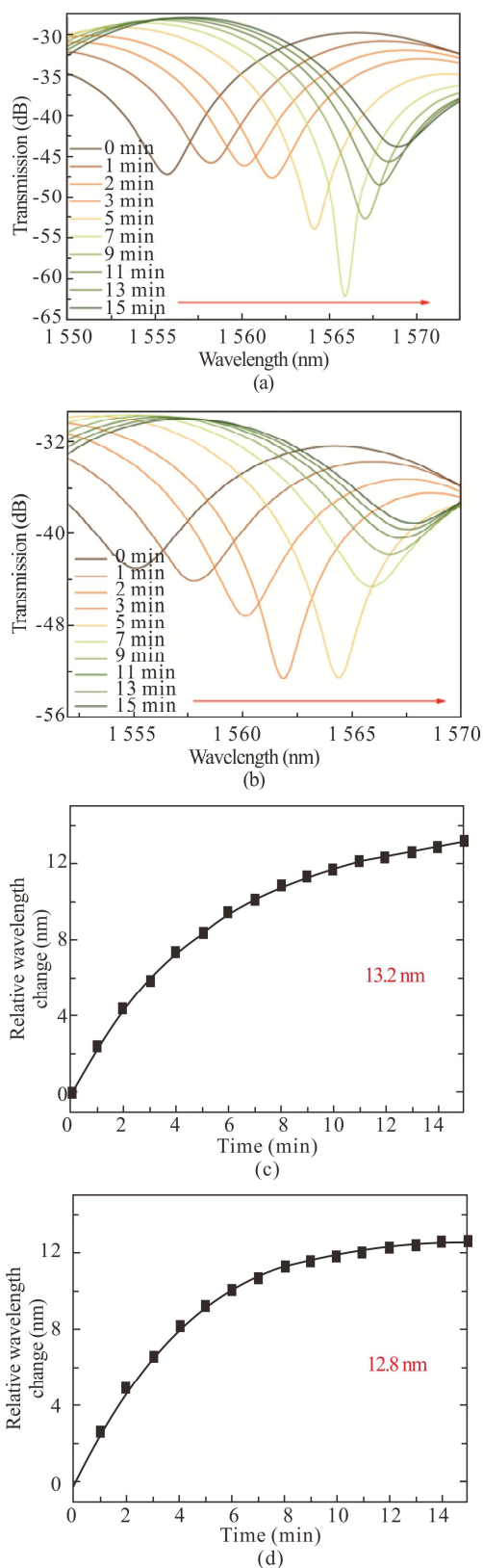


Fig.7 (a) Corresponding transmission spectra and (c) real-time relative wavelength shifts for LOFMZI sensor with another repeated HGFI modification; (b) Corresponding transmission spectra and (d) real-time relative wavelength shifts for LOFMZI sensor with another two repeated HGFI modifications

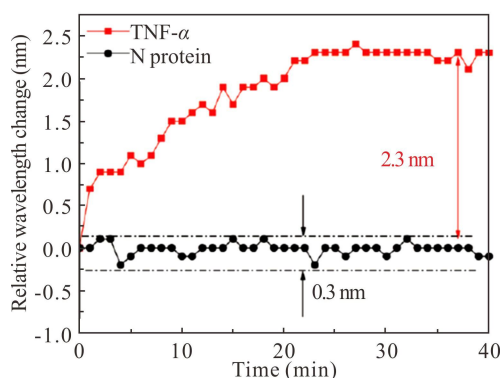


Fig.8 Real-time relative wavelength shifts of an additional detection process for TNF- α and N protein with the LOFMZI sensor

and specific detection of antigen TNF- α with a single sensor by our system. TFA was adopted to remove HGFI which made it accessible to reuse the sensor. Compared with the conventional methods based on electrostatic incorporation and silanisation, our proposed HGFI functionalized LOFMZI sensor presented advantages such as ease of operation, good stability and lower sample consumption, which would serve as a model for more biomarker detection in inflammation and disease monitoring.

Statements and Declarations

The authors declare that there are no conflicts of interest related to this article.

References

- [1] BALKWILL F. TNF- α in promotion and progression of cancer[J]. *Cancer and metastasis reviews*, 2006, 25: 409-416.
- [2] RADNER H, ALETAHA D. Anti-TNF in rheumatoid arthritis: an overview[J]. *Wiener medizinische wochenschrift*, 2015, 165: 3-9.
- [3] DECOURT B, LAHIRI D K, SABBAGH M N. Targeting tumor necrosis factor alpha for Alzheimer’s disease[J]. *Current Alzheimer research*, 2017, 14: 412-425.
- [4] BOSS J D, SINGH P K, PANDYA H K, et al. Assessment of neurotrophins and inflammatory mediators in vitreous of patients with diabetic retinopathy[J]. *Investigative ophthalmology & visual science*, 2017, 58(12): 5594-5603.
- [5] ASIEDU M K, INGLE J N, BEHRENS M D, et al. TGF β /TNF α -mediated epithelial-mesenchymal transition generates breast cancer stem cells with a claudin-low phenotype[J]. *Cancer research*, 2011, 71: 4707-4719.
- [6] RENUKARADHYA G J, EBERLE K C, VENN-WATSON S K, et al. Development and testing of species-specific ELISA assays to measure IFN- γ and TNF- α in bottlenose dolphins (*Tursiops truncatus*)[J]. *Plos one*, 2018, 13(1): e0190786.

- [7] WU H T, WEN Y B, YUE C, et al. Serum TNF- α level is associated with disease severity in adult patients with immunoglobulin a vasculitis nephritis[J]. *Disease markers*, 2020, 2020: 5514145.
- [8] LU Y, ZHOU Q Q, XU L. Non-invasive electrochemical biosensors for TNF- α cytokines detection in body fluids[J]. *Frontiers in bioengineering and biotechnology*, 2021, 9: 701045.
- [9] LUO B B, XU Y F, WU S X, et al. A novel immunosensor based on excessively tilted fiber grating coated with gold nanospheres improves the detection limit of new-castle disease virus[J]. *Biosensors and bioelectronics*, 2018, 100: 169-175.
- [10] DANDAPAT K, TRIPATHI S M, CHINIFOOROSHAN Y, et al. Compact and cost-effective temperature-insensitive bio-sensor based on long-period fiber gratings for accurate detection of *E. coli* bacteria in water[J]. *Optics letters*, 2016, 41(18): 4198-4201.
- [11] EN H Y, WANG S F, LI C H, et al. Real-time and sensitive immunosensor for label-free detection of specific antigen with a comb of microchannel long-period fiber grating[J]. *Analytical chemistry*, 2020, 92: 15989-15996.
- [12] SUN D D, GUO T, RAN Y, et al. In-situ DNA hybridization detection with a reflective microfiber grating biosensor[J]. *Biosensors and bioelectronics*, 2014, 61: 541-546.
- [13] VALADEZ A, LANA C, TU S I, et al. Evanescent wave fiber optic biosensor for salmonella detection in food[J]. *Sensors*, 2009, 9: 5810-5824.
- [14] JAUREGUI-VAZQUEZ D, LOZANO-SOTOMAYOR P, MEJÍA-BENAVIDES J E, et al. Binding analysis of functionalized multimode optical-fiber sandwich-like structure with organic polymer and its sensing application for humidity and beath monitoring[J]. *Biosensors*, 2021, 11(9): 324.
- [15] LINDER M B, SZILVAY G R, NAKARI-SETÄLÄ T, et al. Hydrophobins: the protein-amphiphiles of filamentous fungi[J]. *FEMS microbiology reviews*, 2005, 29: 877-896.
- [16] MGBEAHURUIKE A C, KOVALCHUK A, CHEN H X, et al. Evolutionary analysis of hydrophobin gene family in two wood-degrading basidiomycetes, *Phlebia brevispora* and *Heterobasidion annosum* s.l.[J]. *BMC ecology and evolution*, 2013, 13: 240.
- [17] VRIES O M H, FEKKES M P, WÖSTEN H A B, et al. Insoluble hydrophobin complexes in the walls of *Schizophyllum commune* and other filamentous fungi[J]. *Archives of microbiology*, 1993, 159: 330-335.
- [18] PAANANEN A, VUORIMAA E, TORKKELI M, et al. Structural hierarchy in molecular films of two class II hydrophobins[J]. *Biochemistry*, 2003, 42(18): 5253-5258.
- [19] PISCITELLI A, PENNACCHIO A, LONGOBARDI S, et al. VMH2 hydrophobin as a tool for the development of “self-immobilizing” enzymes for biosensing[J]. *Biotechnology and bioengineering*, 2017, 114: 46-52.
- [20] REUTER L J, SHAHBAZI M A, MÄKILÄ E M, et al. Coating nanoparticles with plant-produced transferin-hydrophobin fusion protein enhances their uptake in cancer cells[J]. *Bioconjugate chemistry*, 2017, 28: 1639-1648.
- [21] FAN H C, WANG B, ZHANG Y, et al. A cryo-electron microscopy support film formed by 2D crystals of hydrophobin HFBI[J]. *Nature communications*, 2021, 12: 7257.
- [22] DUAN S X, WANG B, QIAO M Q, et al. Hydrophobin HGFI-based fibre-optic biosensor for detection of antigen-antibody interaction[J]. *Nanophotonics*, 2019, 9: 177-186.
- [23] SONG B B, JIN C, WANG B, et al. Hydrophobin HGFI assisted immunobiologic sensor based on a cascaded taper integrated ultra-long-period fiber grating[J]. *Biomedical optics express*, 2021, 12(5): 2790-2799.
- [24] WU J X, WANG B, SONG B B, et al. Bioimmunoassay based on hydrophobin HGFI self-assembled whispering gallery mode optofluidic microresonator[J]. *Sensors and actuators A: physical*, 2021, 319: 112545.
- [25] SONG D M, GAO Z D, ZHAO L Q, et al. High-yield fermentation and a novel heat-precipitation purification method for hydrophobin HGFI from *Grifola frondosa* in *Pichia pastoris*[J]. *Protein expression and purification*, 2016, 128: 22-28.
- [26] ZHAO R, SHU X W, WANG P. High-performance bending sensor based on femtosecond laser-inscribed in-fiber Mach-Zehnder interferometer[J]. *Journal of lightwave technology*, 2020, 38: 6371-6378.
- [27] YU F, XUE P, ZHENG J. Enhancement of refractive index sensitivity by bending a core-offset in-line fiber Mach-Zehnder interferometer[J]. *IEEE sensors journal*, 2019, 19: 3328-3334.
- [28] WANG Z F, LIENEMANN M, QIAO M Q, et al. Mechanisms of protein adhesion on surface films of hydrophobin[J]. *Langmuir*, 2010, 26: 8491-8496.